ICASSP 2022 - 2022 IEEE International Conference on Acoustics, Speech and Signal Processing (ICASSP) | 978-1-6654-0540-9/22/$31.00 ©2022 IEEE | DOI: 10.1109/ICASSP43922.2022.9746760

ON THE PREDICTION OF THE FREQUENCY RESPONSE OF A WOODEN PLATE FROM ITS MECHANICAL PARAMETERS

David Giuseppe Badiane, Raffaele Malvermi, Sebastian Gonzalez, Fabio Antonacci and Augusto Sarti

Department of Electronics, Information and Bioengineering,
Politecnico di Milano, Italy

ABSTRACT

Inspired by deep learning applications in structural mechanics, we focus on how to train two predictors to model the relation between the vibrational response of a prescribed point of a wooden plate and its material properties. In particular, the eigenfrequencies of the plate are estimated via multilinear regression, whereas their amplitude is predicted by a feedforward neural network. We show that labeling the train set by mode numbers instead of by the order of appearance of the eigenfrequencies greatly improves the accuracy of the regression and that the coefficients of the multilinear regressor allow the definition of a linear relation between the first eigenfrequencies of the plate and its material properties.

Index Terms— machine learning, musical acoustics, material characterization, feedforward neural network

1. INTRODUCTION

Machine learning has been increasingly employed in the field of structural mechanics, proving to be able to greatly accelerate the characterization of a material [1, 2] and the detection of damages on a solid body [3]. Also musical instruments can benefit from machine learning [4, 5]. In particular, we have started to develop a data-driven approach for musical acoustics, including the definition of a parametric mesh of the violin top plate [6], the use of neural networks to accelerate the prediction of the eigenfrequencies of the violin top [7] and their application for updating-based optimization algorithms [8].

In this article we go beyond the state of the art, showing that a neural network can learn also part of the modal response of a wooden body. By simulating the measurement of a Frequency Response Function (FRF) at prescribed points of a wooden thin plate for varying mechanical parameters, we train a network to estimate not only the eigenfrequencies, but also the magnitude of the modes in the FRF. In particular, the accuracy of the prediction of frequency and magnitude is studied with three datasets differing in the distribution of their input parameters. It is noteworthy that labeling the train set by mode numbers allows to greatly enhance the accuracy of the neural network with respect to the one obtained with a train set sorted by the ascending order of the eigenfrequencies.

We propose the case study of a wooden thin plate of constant geometry since the construction of the guitar family instruments starts from wooden plates of standardized shape. As a result, the first crucial decision of the guitar making process is the selection of a plate with desirable elastic constants [9, 10, 11]. The use of the predictors presented in this paper for optimization tasks opens the door to the use of artificial intelligence powered tools for wood characterization in the workshop of future instrument makers.

The paper is organized as follows: in Sec. 2 an in-depth description of the datasets is provided. In Sec. 3 the predictors are introduced and their results are discussed, both for frequency and amplitude.

2. DATASETS OVERVIEW

One way of characterizing the vibrational behaviour of solids is measuring their point FRF. The point FRF is a frequency domain complex-valued transfer function between an input and an output. Usually, the input is an impulsive force exerted at a given point of the measured body, while the output is the consequent vibration of another point in terms of either displacement, velocity or acceleration. The peaks of the point FRF are the resonances of the body and each of these is associated to an eigenfrequency and a modal shape, which describes how the body vibrates at resonance.

In this work we focus on the point FRF measured at prescribed points of the wooden plate with fixed dimensions $(451 \times 190 \times 3.5)\mathrm{mm}$ shown in the left part of Figure 1. In the right part of Figure 1 an example of a point FRF is shown along with the associated modal shapes. Dark red areas correspond to the nodal lines (i.e. lines of zero displacement) characterizing the specific mode. The magnitude of the FRF at the eigenfrequencies is proportional to the product of the modal shape evaluated at the measurement points [12]. Since the geometry of each modal shape depends from the plate material properties, the relation between the material properties and the magnitude of the FRF peaks is strongly nonlinear.

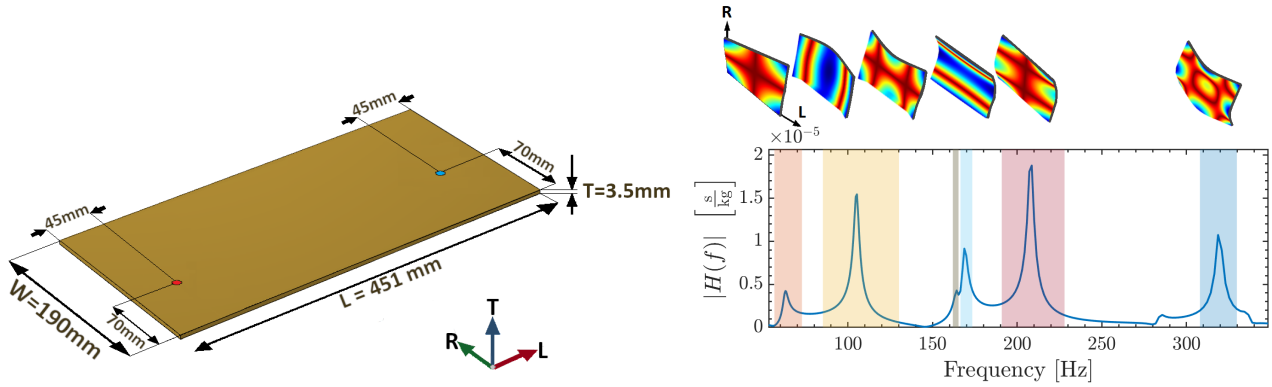

Fig. 1. **Left:** 3D model of the plate simulated to generate the datasets. The red and blue circles represent the excitation point and the measurement point, where an impact force is exerted and the velocity of the point is retrieved, respectively. The plate is in free boundary conditions. **Right:** simulated point Frequency Response Function (FRF) of the plate for the nominal values shown in Table 1. The modes depicted in the figure are, from left to right: $(1,1)$, $(0,2)$, $(1,2)$, $(2,0)$, $(2,1)$, $(2,2)$. The amplitude associated to each eigenfrequency is proportional to the product of the modal shape evaluated at the measurement points.

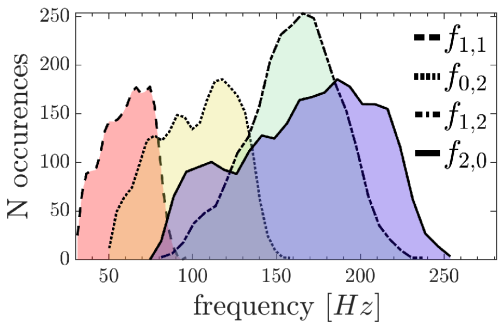

Fig. 2. Histogram depicting the distribution of the first four eigenfrequencies $f_{(1,1)}$, $f_{(0,2)}$, $f_{(1,2)}$ and $f_{(2,0)}$ in the U_{75} dataset. The modes will not always appear in the same order inside the point FRF, as a result the curves are partially overlapped. In particular $f_{(2,0)}$ is the most varying eigenfrequency as it displays the widest range and overlaps with all the other modes.

We develop the train sets by simulating the value of the first four peaks of the point FRF of the plate as the material parameters vary. In this regard, since wood is an orthotropic material, ten mechanical parameters are needed to characterize its elastic properties. Namely, we use three Young's moduli, three Shear moduli, three Poisson's Ratios, and the density. Moreover, we characterize its damping by means of the Rayleigh damping model [13] and randomly sample the control variables of the model, α and β, thus including two additional input parameters. We use for our simulations the nominal elastic constants of Sitka spruce [14] shown in Table 1 and let the parameters vary around them. For each occurrence of the dataset the eigenfrequencies, the modal shapes and the peak values of the point FRF are computed with *Comsol Multiphysics®* .

The instances in the dataset are randomly sampled from: a Gaussian distribution centered on the nominal values, whose standard deviation is 10% of the mean (dataset G_{10}); and two uniform distributions centered around the nominal values with their span set to 50% and 75% of the mean, yielding the U_{50} and U_{75} datasets, respectively. Each of the three datasets contains $N = 2500$ samples.

Notice that the ordering in which the modes appear along the frequency axis changes as the mechanical parameters vary [15]. Figure 2 shows the distribution of the eigenfrequencies on the frequency axis for the dataset U_{75}. It is clearly visible that a strong overlap between the distributions exists, generating the change of order in the frequency associated to the modes. Each eigenfrequency has a particular distribution profile: while $f_{(1,1)}$ distribution is quite narrow, the one related to $f_{(2,0)}$ is the largest and intersects all the other ones. Indeed, in our case study the mode $(2,0)$ is usually associated to the fourth peak of the point FRF, but for given values of the input parameters it can correspond to the second.

In order to avoid outliers and reduce noise in the regression, we perform a preliminary identification of the modal shapes by comparing them to a reference set of modal shapes obtained for the nominal values of Sitka spruce and labelled by mode numbers. The similarity between the resulting modal shapes $\hat{\mathbf{\Phi}}$ and the reference set $\mathbf{\Phi}$ is evaluated in terms of Normalized Cross Correlation (NCC), which is computed as $\mathrm{NCC}(\hat{\mathbf{\Phi}}, \mathbf{\Phi}) = \frac{\hat{\mathbf{\Phi}}^T \mathbf{\Phi}}{\|\hat{\mathbf{\Phi}}\|_2 \|\mathbf{\Phi}\|_2}$. Each modal shape $\hat{\mathbf{\Phi}}$ is then labelled with the reference mode scoring the maximum NCC value. As a last step, all the occurrences of the dataset displaying either repeated modes or an $NCC < 0.9$ for at least one mode are discarded.

Young's Moduli	Shear Moduli	Poisson's Ratios
$E_{L_0} = 10.8$ [GPa]	$G_{LR_0} = 0.061E_{L_0}$	$\nu_{LR} = 0.467$
$E_{R_0} = 0.043E_{L_0}$	$G_{RT_0} = 0.064E_{L_0}$	$\nu_{RT} = 0.372$
$E_{T_0} = 0.078E_{L_0}$	$G_{LT_0} = 0.003E_{L_0}$	$\nu_{LT} = 0.435$

Table 1. Nominal values of the mechanical parameters of Sitka spruce, which is commonly employed for the soundboards of stringed instruments [16]. Damping is modeled through Rayleigh damping. The central values of the damping constants are $\alpha_0 = 19$ and $\beta_0 = 10^{-6}$. The mean value of the density comes from measurements on a real plate with the same geometry and is $\rho_0 = 400kg/m^3$.

3. RESULTS

The datasets are employed to train two predictors, a Multiple Linear Regressor (MLR) [17] for the eigenfrequencies and a Multilayer Feedforward Neural Network (MFNN) [18] for the magnitude. The quality of the estimation provided by both the models is assessed by evaluating the coefficient of determination R^2, which provides a measure of how accurately the model replicates the observed outcomes [19, 20]. We evaluate the average coefficient of determination defined as

$$\overline{R^2} = \frac{1}{4}\sum_{i=1}^{4} R^2_{m_i}\,, \quad \mathbf{m} = [(1,1),(0,2),(2,1),(2,0)] \quad (1)$$

which takes into account the first four modes of the plate, either for frequency or amplitude.

3.1. Frequency

The dataset G_{10} is randomly split into test set (10% of the samples) and train set (90% of the samples) to study the regression accuracy of the MLR. As a first step, we train the MLR with and without ordering the train set by modes and perform an F-test [21]. Testing the MLR for $f_{(2,0)}$ yields $R^2_{(2,0)} = 0.994$, $F\text{-}stat_{(2,0)} = 3228$ and $p\text{-}value_{(2,0)} \approx 0$. Instead, if we use the fourth peak in ascending order, we get $R^2_{(4)} = 0.921$, $F\text{-}stat_{(4)} = 369$ and $p\text{-}value_{(4)} \approx 0$. The low p-values indicate that both regressors are statistically significant, whereas the higher F-statistic and R^2 relative to $f_{(2,0)}$ imply that ordering the dataset by modes enhances the expressivity and the accuracy of the model.

Replicating the same splitting into test and train sets on the three labelled datasets, the average coefficients of determination are $\overline{R^2} = 0.993$ for the G_{10}, $\overline{R^2} = 0.990$ for the U_{50} and $\overline{R^2} = 0.983$ for the U_{75}. We can conclude that MLR is a reliable estimation technique for the plate eigenfrequencies regardless of the distribution characterizing the dataset.

The coefficients of the MLR can be used to obtain relations between the elastic constants E_L, E_R, G_{LR} and the eigenfrequencies $f_{(0,2)}$, $f_{(2,0)}$, $f_{(1,1)}$. We can approximate the eigenfrequencies as linear combinations of the density and one of the mechanical parameters that we want to infer. Thus, we obtain a system of three equations and three unknowns which can be easily inverted as

$$\begin{cases} E_L &\approx a_1 + 10^6\left(b_1\rho + c_1 f_{(0,2)}\right) \\ E_R &\approx a_2 + 10^6\left(b_2\rho + c_2 f_{(2,0)}\right) \\ G_{LR} &\approx a_3 + 10^6\left(b_3\rho + c_3 f_{(1,1)}\right) \end{cases}, \quad (2)$$

where ρ is the plate density, $f_{(m,n)}$ are the signature eigenfrequencies and the elastic constants E_L, E_R, G_{LR} are expressed in MPa. The weights of eq. (2) have the following values and unit measures:

$$\underline{\mathbf{a}} = \begin{bmatrix} -29000 \\ -2150 \\ -1850 \end{bmatrix} \text{MPa}, \quad \underline{\mathbf{b}} = \begin{bmatrix} 35.6 \\ 2.71 \\ 2.35 \end{bmatrix} \frac{\text{m}^2}{\text{s}^2}, \quad \underline{\mathbf{c}} = \begin{bmatrix} 274 \\ 12.9 \\ 29.3 \end{bmatrix} \frac{\text{kg}}{\text{m s}}.$$

The relation above is obtained with the coefficients of the MLR trained with the G_{10} dataset.

Notice that similar equations have been proposed by Caldersmith in [22], i.e. eqs. (7) to (9). Caldersmith's formulas and the ones in eq. (2) are tested on the whole G_{10} dataset. We assess the quality of the two estimators by evaluating the Mean Absolute Percentage Error (MAPE), which is computed as

$$\text{MAPE} = 100\,\frac{1}{I}\sum_{i=1}^{I}\left|\frac{y-\hat{y}}{y}\right|, \quad (3)$$

where y is the target, $\hat{y}$ is the prediction of the model and $I = 2500$ is the number of observations. While for Caldersmith's formulas we have a MAPE of 0.88% on E_L, 3.38% on E_R and 11.77% on G_{LR}, with eq. (2) we obtain 0.35% on E_L, 1.99% on E_R and 9.22% on G_{LR}, thus achieving a good improvement. Nevertheless, further investigations are needed in order to establish whether this improvement holds for plates of different geometry.

3.2. Amplitude

Since the input/output relation between material parameters and amplitudes is strongly nonlinear, we need a more flexible model, such as a feedforward neural network. In this paper the *Matlab*® Machine Learning Toolbox (NNTRAINTOOL) is used to implement, train and validate the network following the Levemberg-Marquadt algorithm. The activation function and the loss function employed are the logistic sigmoid function and the mean squared error, respectively. Each neural network is trained for 1000 epochs with early stopping. A detailed description of the toolbox can be found in [23, 24].

A diagram of a feedforward neural network is depicted in the left part of Figure 3. The total number of layers $\mathcal{L}$ and the number of neurons per hidden layer $\mathcal{M}$ define the topology of the MFNN. We tune the hyperparameters of the neural network carrying out a grid search varying $\mathcal{M}$ and $\mathcal{L}$ and evaluating each time the mean coefficient of determination defined

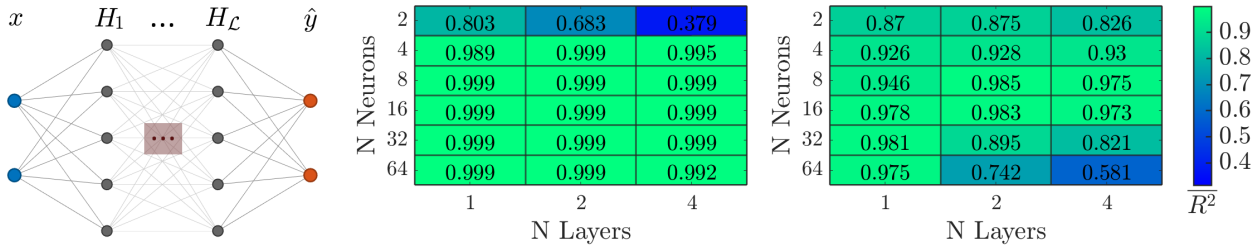

Fig. 3. **Left**: diagram of a feedforward neural network. The one depicted in the figure has two inputs in the input layer x, two outputs in the output layer $\hat{y}$ and $\mathcal{L}$ hidden layers H of five neurons each. **Center**: hyperparameters tuning of the network trained with the G_{10} dataset. **Right**: hyperparameters tuning of the network trained with the U_{75} dataset. The matrices show the mean coefficient of determination $\overline{R^2}$ defined in eq. (1) associated to the estimation of the amplitude relative to the eigenfrequencies $f_{(1,1)}$, $f_{(0,2)}$, $f_{(2,1)}$, $f_{(2,0)}$.

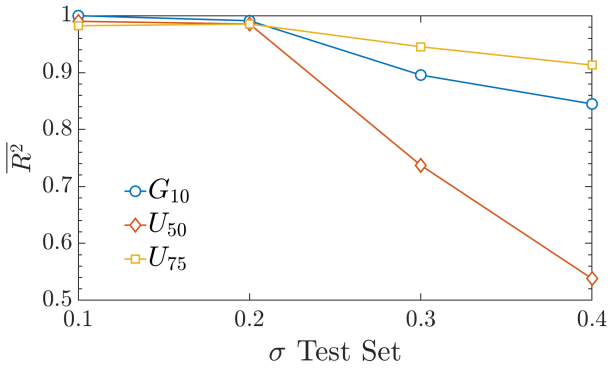

Fig. 4. Mean coefficient of determination $\overline{R^2}$, defined in eq. (1), relative to the prediction of the amplitudes performed by the feedforward neural network. The model is trained with the three datasets and tested on four normally distributed test sets G_σ with increasing standard deviation, that goes from $\sigma = 0.1$ to $\sigma = 0.4$ with a step of 0.1.

in eq. (1) on a Gaussian test set with $\sigma = 0.1$ containing 250 tuples never seen by the models.

Figure 3 shows the results of the hyperparameters tuning relative to the G_{10} and the U_{75}. The low $\overline{R^2}$ values in the right-bottom part of the matrices are caused by overfitting, as the neural networks display a low and decreasing loss in the training, whereas the loss relative to testing remains high and constant (data not shown). One hidden layer and eight neurons are enough to obtain $\overline{R^2} = 0.999$ when training with the G_{10}. Given the accuracy of the network, there is no need to further optimize the architecture. On the other side, since the U_{75} is way broader, two layers and eight neurons yield the best model, with an $\overline{R^2} = 0.985$.

In order to evaluate how the networks estimate observations that fall outside the span of their training set, the neural networks are tested with four G_σ test sets of 100 occurrences each. The G_σ test sets are all normally distributed around the nominal values shown in Table 1 with a standard deviation that goes from $\sigma = 0.1$ to $\sigma = 0.4$, with a step of 0.1.

Figure 4 shows the mean coefficient of determination $\overline{R^2}$ for the testing process mentioned above. As the standard deviation of the test set increases, the $\overline{R^2}$ associated to the MFNN trained with the U_{75} overcomes the one relative to the network trained with the G_{10}. Nevertheless, the mean coefficient of determination of G_{10} remains comparable to the one of the U_{75}, even if the distribution of the input parameters in the G_{10} is thinner than in U_{75} and U_{50}. This suggests that the network trained with the G_{10} has effectively learned to generalize the relation between the material parameters and the magnitude of the modes inside the FRF. On the other hand, the network trained on the U_{50} presents the worst generalization ability as its accuracy abruptly decreases whenever the span of the G_σ test set overcomes the one of the U_{50}.

4. CONCLUSIONS

This paper studies how to train two predictors to estimate the point FRF evaluated at the eigenfrequencies of a wooden plate. In particular, the eigenfrequencies and their amplitude are estimated by a multilinear regressor and a feedforward neural network, respectively.

To the best of our knowledge, this is the first time that the dependance between the order of appearance of the eigenfrequencies and the material parameters is studied. In particular, the variability of the material properties causes a switching in the order of appearance of modes. In this direction, we showed that using the mode numbers instead of the order of appearance of modes to label the train set allows to greatly enhances the regression accuracy, regardless of the distribution (normal or uniform, wide or thin) of the train set inputs.

Moreover, the MLR provides a linear relation between the material parameters and the first eigenfrequencies of the plate that is, for our plate, more accurate with respect to the ones presented in the literature [22, 25, 26], which are still used to estimate the elastic constants of wooden plates.

5. REFERENCES

[1] Frederic E. Bock, Roland C. Aydin, Christian J. Cyron, Norbert Huber, Surya R. Kalidindi, and Benjamin Klusemann, "A review of the application of machine learning and data mining approaches in continuum materials mechanics," *Frontiers in Materials*, vol. 6, 2019.

[2] Hamidreza Fathi, Vahid Nasir, and Siavash Kazemirad, "Prediction of the mechanical properties of wood using guided wave propagation and machine learning," *Construction and Building Materials*, vol. 262, 2020.

[3] Onur Avci, Osama Abdeljaber, Serkan Kiranyaz, Mohammed Hussein, Moncef Gabbouj, and Daniel J. Inman, "A review of vibration-based damage detection in civil structures: from traditional methods to machine learning and deep learning applications," *Mechanical Systems and Signal Processing*, vol. 147, 2021.

[4] Marco Olivieri, Raffaele Malvermi, Mirco Pezzoli, Massimiliano Zanoni, Sebastian Gonzalez, Fabio Antonacci, and Augusto Sarti, "Audio information retrieval and musical acoustics," *IEEE Instrumentation & Measurement Magazine*, vol. 24, no. 7, pp. 10–20, 2021.

[5] Matteo Acerbi, Raffaele Malvermi, Mirco Pezzoli, Fabio Antonacci, Augusto Sarti, and Roberto Corradi, "Interpolation of irregularly sampled frequency response functions using convolutional neural networks," in *ICASSP 2021-2021 IEEE International Conference on Acoustics, Speech and Signal Processing (ICASSP)*. IEEE, 2021, pp. 950–954.

[6] Sebastian Gonzalez, Davide Salvi, Fabio Antonacci, and Augusto Sarti, "Eigenfrequency optimisation of free violin plates," *The Journal of the Acoustical Society of America*, vol. 149, no. 3, pp. 1400–1410, 2021.

[7] Sebastian Gonzalez, Davide Salvi, Daniel Baeza, Fabio Antonacci, and Augusto Sarti, "A data-driven approach to violin making," *Scientific reports*, vol. 11, no. 1, pp. 1–9, 2021.

[8] Davide Salvi, Sebastian Gonzalez, Fabio Antonacci, and Augusto Sarti, "Parametric optimization of violin top plates using machine learning," *arXiv preprint arXiv:2102.07133*, 2021.

[9] E. Obataya, T Ono, and M Norimoto, "Vibrational properties of wood along the grain," *Journal of Materials Science*, vol. 35, no. 12, pp. 2993–3001, 2000.

[10] Capucine Carlier, Ahmad Alkadri, Joseph Gril, and Iris Bremaud, "Revisiting the notion of "resonance wood" choice: a decompartementalised approach from violin makers' opinion and perception to characterization of material properties variability," *Wooden musical instruments - Different forms of knowledge: Book of end of WoodMusICK COST Action FP1302*, pp. 119–142, 2018.

[11] Ennio Hugo Idrobo-Ávila and Rubiel Vargas-Cañas, "Acoustic and mechanic characterization of materials used in manufacturing the soundboard of the spanish guitar: Influence in the sonority," *Revista Facultad de Ingeniería Universidad de Antioquia*, , no. 76, pp. 30–38, 2015.

[12] Leonard Meirovitch, *Fundamentals of Vibrations*, Waveland Press, 2010.

[13] John William Strutt Rayleigh, *The Theory of Sound, Volume One*, Dover Books on Physics. Dover Publications, 2013.

[14] Forest Products Laboratory (US), *Wood Handbook: Wood as an Engineering Material*, The Laboratory, 1987.

[15] Peter Persson, Ola Flodén, Henrik Danielsson, Andrew Peplow, and Lars Vabbersgaard Andersen, "Improved low-frequency performance of cross-laminated timber floor panels by informed material selection," *Applied Acoustics*, vol. 179, 2021.

[16] Ulrike G.K. Wegst, "Wood for sound," *American Journal of Botany*, vol. 93, no. 10, pp. 1439–1448, 2006.

[17] Mark Tranmer and Mark Elliot, "Multiple linear regression," *The Cathie Marsh Centre for Census and Survey Research (CCSR)*, 2008.

[18] Daniel Svozil, Vladimir Kvasnicka, and Jiri Pospichal, "Introduction to multi-layer feed-forward neural networks," *Chemometrics and intelligent laboratory systems*, vol. 39, no. 1, pp. 43–62, 1997.

[19] Stanton Glantz and Bryan Slinker, *Primer of Applied Regression & Analysis of Variance, 3rd edition*, McGraw-Hill, Inc., New York, 2001.

[20] Norman R. Draper and Harry Smith, *Applied Regression Analysis*, vol. 326, John Wiley & Sons, 1998.

[21] Kurt Schmidheiny and Unversität Basel, "The multiple linear regression model," *Short Guides to Microeconometrics, Version*, vol. 20, 2013.

[22] Graham Caldersmith and Freeman Elizabeth, "Wood properties from sample plate measurements i," *Journal of Catgut Acoustic*, vol. 1, no. II, pp. 8–12, 1990.

[23] Mark Hudson Beale, Martin T. Hagan, and Howard B. Demuth, "Neural network toolbox user's guide," *The MathWorks Inc.*, vol. 103, 1992.

[24] Fadi Aldakheel, Ramish Satari, and Peter Wriggers, "Feed-forward neural networks for failure mechanics problems," *Applied Sciences*, vol. 11, no. 14, pp. 6483, 2021.

[25] Michael Mclntyre and Jim Woodhouse, "On measuring wood properties, part 2," *Journal Catgut Acoustical Society*, vol. 43, pp. 18–24, 1985.

[26] Graham Caldersmith, "Vibrations of orthotropic rectangular plates," *Acta Acustica united with Acustica*, vol. 56, no. 2, pp. 144–152, 1984.